

TABLE I. Boundary recombination velocities for several specimens.

Spec. no.	Resistivity, $\rho$ ohm-cm	Body lifetime, $\tau$ $\mu$ sec	Crystal boundary recombination velocity, $v$ cm/sec
A	16 - $n$	1100	$2.0 \times 10^8$
B	9.0 - $n$	450	1.2
C	7.1 - $n$	310	2.6
D	3.0 - $p$	250	1.6

and in the edge orientation, are spaced at intervals of about a micron.

The recombination was studied by the Morton-Haynes<sup>4</sup> method, illustrated in Fig. 1(a). The (movable) light source generates excess carriers and their concentration is measured as a function of the position  $x_l$  of the light source. In an  $n$ -type specimen the excess hole concentration at the (fixed) collector point is proportional to the collector current which is measured as the voltage,  $V$ , across a resistor in series with the collector. The straight-line portion of the  $V$  vs  $x_l$  plot gives body lifetime. Figure 1(b) shows  $V$  vs  $x_l$  for a fixed position,  $x_b$ , of the grain boundary. As the light approaches the grain boundary, the slope of the  $V$  vs  $x_l$  curve becomes steeper—indicating that the boundary is a sink for holes; that is, a greater fraction of the light-generated holes moves to the right, or toward the boundary, rather than to the left, or toward the collector.

At the top in Fig. 1(a) are the solutions to the diffusion equation giving the excess hole concentration  $\delta p(x)$  in the three regions shown. The bulk diffusion length is taken as unit length.  $A_1, A_2, B_2, B_3$  are functions of  $x_l$  and  $x_b$ , and are determined by the following boundary conditions:  $\delta p(x)$  is continuous at  $x_l$  and  $x_b$ ; the discontinuity in hole current at  $x_l$  is the rate of hole generation and the discontinuity at  $x_b$  is  $v\delta p(x_b)$ , where  $v$  is the recombination velocity. Using the fact that  $\delta p$  at the collector ( $x=0$ ) is proportional to  $V$ , we find

$$\ln[1 - (V/V_0)] + \ln[(2v_1/v) + 1] = -2(x_b - x_l),$$

where  $V_0$  is the potential that would be observed in the absence of the grain boundary and  $v_1 = (\text{diffusion length})/(\text{lifetime})$  in the bulk material. When the light is 40 or more mils to the left of the

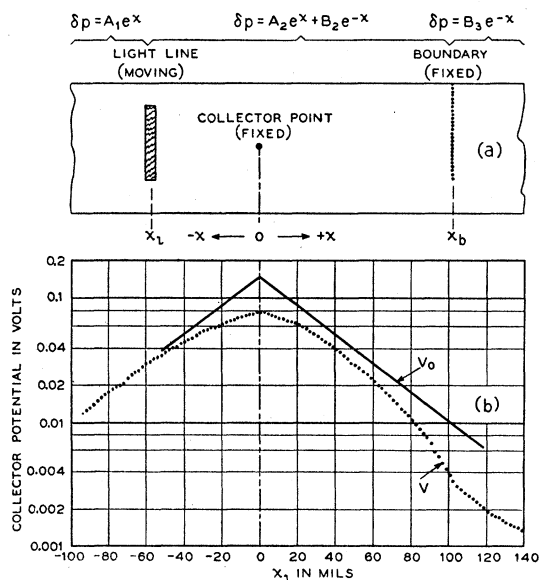


FIG. 1 (a) Diagram of the positions of the fixed collector point and grain boundary and the movable light line on an  $n$ -type specimen. At the top of the figure are the solutions of the diffusion equation for excess hole concentration  $\delta p$  vs distance  $x$  from the collector in the three regions indicated. (b) The collector potential plotted as a function of the position  $x_l$  of the movable light line for specimen B.

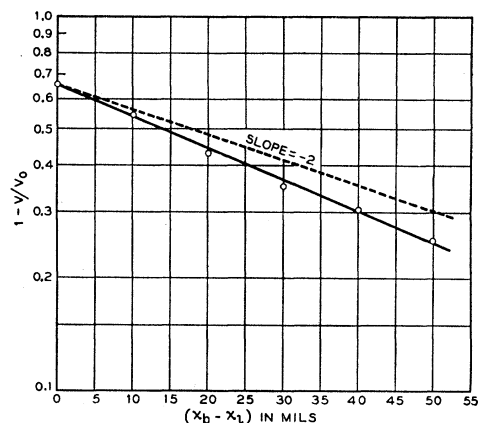


FIG. 2. Plot of  $1 - (V/V_0)$  versus  $(x_b - x_l)$ , where  $V$  is collector potential and  $V_0$  is the potential that would be observed in the absence of a grain boundary. Both  $V$  and  $V_0$  are found from Fig. 1(b). The theory predicts a straight line of slope  $-2$ .

collector, the points in Fig. 1(b) fall on a straight line, which reflected about  $x=0$  gives  $V_0$  for corresponding positions of the light to the right of the collector. Figure 2 shows a semilog plot of  $[1 - (V/V_0)]$  vs  $(x_b - x_l)$ . The points are well fitted by a straight line of slope  $-2$ . The intercept at  $x_b - x_l = 0$  gives  $v$ . Comparable agreement with the theory was obtained for three other specimens. Table I gives the resistivity, conductivity type, lifetime, and recombination velocity for the four specimens.

The existence of a surface recombination velocity at the crystal boundary indicates a concentration of recombination centers in the boundary. The density of these centers cannot, however, be calculated from the data because of uncertainties in (1) the carrier concentration in the space-charge region at the boundary, (2) the capture cross section, and (3) the number of traps which are charged.

- <sup>1</sup> Vogel, Pfann, Corey, and Thomas, Phys. Rev. **90**, 489-489 (1953).
- <sup>2</sup> W. Shockley, Phys. Rev. **91**, 228 (1953).
- <sup>3</sup> Pearson, Read, and Morin, Phys. Rev. **93**, 666 (1954).
- <sup>4</sup> L. B. Valdes, Proc. Inst. Radio Engrs. **40**, 1420 (1952).

## Magnetic Anisotropy of NiF<sub>2</sub>

L. M. MATARRESE AND J. W. STOUT  
*Institute for the Study of Metals and Department of Chemistry,  
 The University of Chicago, Chicago, Illinois*  
 (Received April 26, 1954)

IN an investigation of the magnetic anisotropy of a single crystal of NiF<sub>2</sub> we have observed phenomena which are unlike those found<sup>1,2</sup> in the isomorphous substances MnF<sub>2</sub>, FeF<sub>2</sub>, and CoF<sub>2</sub>, and which lead us to believe that below the Curie temperature a small ferromagnetic moment appears in NiF<sub>2</sub>. In a normal paramagnetic or antiferromagnetic substance the magnetic susceptibility may be represented by a second-order tensor and in this case the torque on a single crystal in a uniform magnetic field is proportional to the square of the field strength and to the sine of twice the angle between the field direction and the direction of maximum susceptibility in the plane of rotation. Such a behavior was observed for NiF<sub>2</sub> at temperatures above the maximum in heat capacity<sup>3</sup> occurring at 73.2°K. The single crystal was oriented so that the plane of rotation contained the tetragonal [001] axis and a [110] direction. Unlike the other isomorphous fluorides, the susceptibility of NiF<sub>2</sub> at room temperature was greater perpendicular to the tetragonal axis than parallel to it and the difference between the perpendicular and parallel molar susceptibilities rose gradually from  $1.102 \times 10^{-4}$  at 301.15°K to  $1.890 \times 10^{-4}$  at 90.07°K. Below 73.2°K the observed torques were large and anomalous in their dependence on field strength and angle. The torque measured

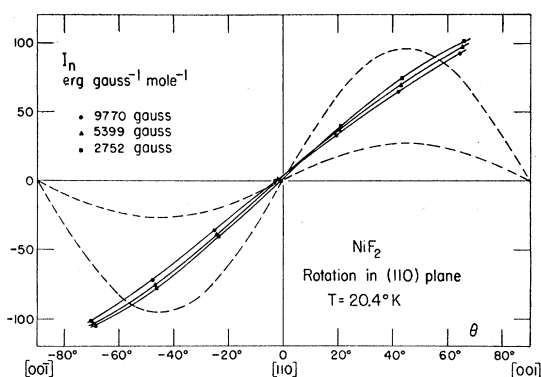


FIG. 1. Molal perpendicular magnetization of nickel fluoride versus angle between field and  $[110]$  direction. Rotation in  $(110)$  plane. Dashed curves indicate typical antiferromagnetic behavior.

by the torsion balance<sup>4</sup> is proportional to  $I_n$ , the component of the magnetization which is perpendicular both to the field direction and to the axis of the suspension. In Fig. 1 are shown values of  $I_n$  at  $20.4^\circ\text{K}$  and for three field strengths. The observed torques were identical at positions  $180^\circ$  from one another. The dashed curves in Fig. 1 illustrate the behavior expected for an antiferromagnetic substance with no permanent moment and a susceptibility independent of field strength. In this case  $I_n$  is proportional to the field strength and the two dashed curves correspond to 2752 and 9770 gauss. The magnitude of the dashed curves is calculated from the powder susceptibility data of de Haas, Schultz, and Koolhaas<sup>5</sup> at  $20.4^\circ\text{K}$ , assuming that the susceptibility parallel to the tetragonal axis is essentially zero. The observed values of  $I_n$  vary little with field strength and are suggestive of that expected from a permanent moment whose projection in the  $(110)$  plane lies preferentially in a  $[110]$  direction but which can be rotated somewhat from this position by a magnetic field.

Measurements were then made of the torques with the crystal mounted so its tetragonal axis was parallel to the axis of the suspension. In this orientation no torques are expected for a normal paramagnetic or antiferromagnetic crystal and only very small ones, amounting to 1.5 percent of the torques in the first orientation and attributable to a misorientation of a small portion of the crystal, were found above  $73.2^\circ\text{K}$ . Below this temperature, however, large torques were observed in this second orientation. These torques had a periodicity of  $90^\circ$ . Values of  $I_n$  at  $20.4^\circ\text{K}$  are shown in Fig. 2. These curves may be fitted by a model<sup>6</sup> such as is used to interpret ferromagnetic anisotropy. In the  $(110)$  plane the easy directions of magnetization are  $\langle 100 \rangle$ . The moment

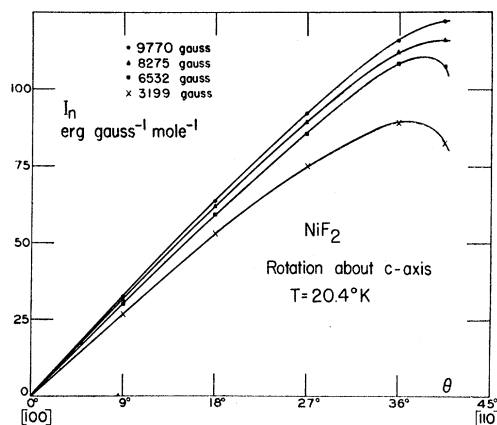


FIG. 2. Molal perpendicular magnetization of nickel fluoride versus angle between field and  $[100]$  direction. Rotation about tetragonal axis.

is assumed constant in magnitude and its direction is determined by the balance between the torque exerted by the magnetic field and that arising from the crystal anisotropy which will have a periodicity of  $90^\circ$ . The curves are consistent with a permanent moment whose magnitude is about  $350 \text{ erg gauss}^{-1} \text{ mole}^{-1}$ . However, the crystalline anisotropy "constant" turns out to increase slightly more than proportionally to the field strength. The reason for this is obscure and there is therefore some question as to the applicability of the usual model for ferromagnetic anisotropy to  $\text{NiF}_2$ .

Erickson<sup>7</sup> has observed in neutron diffraction measurements on  $\text{NiF}_2$  a small peak which was not found in the other antiferromagnetic fluorides of the iron group and which he interpreted as indicating that in the ordered alignment the spins, instead of being strictly parallel and antiparallel to the tetragonal axis as in  $\text{MnF}_2$ ,  $\text{FeF}_2$ , and  $\text{CoF}_2$ , are in  $\text{NiF}_2$  inclined at an angle of  $10^\circ$  from this axis. If one assumes that the cocking of one sublattice is in the  $[110]$  direction and that of the other sublattice at right angles in the  $[1\bar{1}0]$  direction, then there is a net moment in the  $[100]$  direction. The moment of  $350 \text{ erg gauss}^{-1} \text{ mole}^{-1}$ , which is 3 percent of the saturation moment of the nickel ions, would on such a model correspond to a cocking of  $2.5^\circ$ .

The crystal used for the measurements weighed 17 mg and contained impurities of 0.02 percent Co; 0.02 percent Fe; 0.01 percent Al; 0.005 percent Cu; and 0.001 percent Mn, Mg, and Si. In order to see if the observed effects were dependent on the impurity content, some measurements were made on a large crystal containing about 1 percent Fe. The magnetizations observed below the Curie temperature with this impure crystal agreed within 0.7 percent with those found with the small purer crystal, so we do not believe that impurities are the cause of the observed phenomena.

<sup>1</sup> M. Griffel and J. W. Stout, *J. Chem. Phys.* **18**, 1455 (1950).

<sup>2</sup> J. W. Stout and L. M. Matarrese, *Revs. Modern Phys.* **25**, 338 (1953).

<sup>3</sup> J. W. Stout and E. Catalano, *Phys. Rev.* **92**, 1575 (1953).

<sup>4</sup> J. W. Stout and M. Griffel, *J. Chem. Phys.* **18**, 1449 (1950).

<sup>5</sup> de Haas, Schultz, and Koolhaas, *Physica* **7**, 57 (1940).

<sup>6</sup> See F. Bitter, *Introduction to Ferromagnetism* (McGraw-Hill Book Company, Inc., New York, 1937), Chap. VI; R. M. Bozorth, *Ferromagnetism* (D. Van Nostrand Company, Inc., New York, 1951), Chap. 12.

<sup>7</sup> R. A. Erickson, *Phys. Rev.* **90**, 779 (1953).

## Radiogenic Argon Measurements

H. A. SHILLIBEER, R. D. RUSSELL, R. M. FARQUHAR, AND E. A. W. JONES  
*Geophysics Laboratory, Department of Physics, University of Toronto,  
Toronto, Canada*

(Received April 14, 1954)

SOME of the writers recently published the results of an experiment to determine the branching ratio of potassium by the extraction and measurement of radiogenic argon from dated potassium minerals.<sup>1</sup> The value of 0.06 obtained in this way is appreciably lower than the value obtained in many recent gamma-ray counting experiments. Errors in our experiment could have arisen from loss of argon during the purification process, incomplete extraction of the argon from the minerals, or incorrect dating of the minerals.

We have since carried out a number of yield runs in the purification apparatus and found that in all cases no measurable loss occurred. The argon extractions had been carried out by heating the sample to  $850^\circ\text{C}$  in vacuum with a sodium metal flux. To test the efficiency of this procedure we sent a second sample of Bessner microcline to G. J. Wasserburg at the University of Chicago who

TABLE I. Comparison of fluxes.

Locality	$A^{40}/K^{40}$			
	Sodium flux		Sodium hydroxide flux	
	Result	No. of runs	Result	No. of runs
Varala, Finland	0.119	2	0.140	6
Lee Lake, Saskatchewan	0.087	3	0.131	2
Dill Township, Ontario	0.0421	3	0.0522	6